ASSESSMENT OF THERMAL CONDITIONS IN KRASNOYARSK URBAN AREA WITH USE OF DIFFERENT SATELLITE DATA AND GEOGRAPHIC INFORMATION SYSTEM

by

Alexandra K. MATUZKO[a] and Oleg E. YAKUBAILIK[a,b*]

[a]Institute of Computational Modelling of the Siberian Branch of the Russian Academy of Science, Krasnoyarsk, Russia
[b]Siberian Federal University, Krasnoyarsk, Russia

Original scientific paper
https://doi.org/10.2298/TSCI19S2615M

Satellite data in the thermal infrared range are a powerful source of information for the analysis and determination of city urban area temperature anomalies. The article presents a technique for monitoring the land surface temperature on the basis of combination of "Landsat 8" satellite thermal infrared data with PlanetScope satellite constellation high resolution data. Such combination of satellite data from several spacecrafts increase the detalization of temperature maps to the level of individual city blocks. Determination of the nature and boundaries of temperature anomalies will help to understand the causes of the unfavorable environmental situation in Krasnoyarsk, where, in addition to high industrial emissions, their influence and atmospheric processes, leading to the fact that impurities are delayed and concentrated over the city. The results shows that the temperature in the places of thermal anomalies is 5º-8º higher than the average land surface temperature of the city. Based on the results of the analysis of summer thermal multi-temporal space images, several thermal zones of different nature were outlined on the territory under consideration. This information can be used in planning the development of the city, the design of new urban neighborhoods.

Key words: thermal satellite images, urban heat island, infrared image, land surface temperature, Landsat

Introduction

Temperature is one of the key indicators of the natural environment. It can be measured by ground-based methods or using satellite remote sensing data. Satellite remote sensing has become a worthy alternative to traditional methods of temperature measurement in the context of a highly sparse and even shrinking network of terrestrial weather stations in recent years. A very important characteristic of remote sensing is the possibility of obtaining a long-term homogeneous series of land surface temperature (LST) data [1].

Recently, special attention is paid to the urban heat islands (UHI) [2-4]. We are talking about an increase in the ambient temperature observed in large cities, where the air temperature usually is several degrees higher than in the adjacent areas [5, 6]. Studies carried out in different countries show that this effect is observed in almost all major cities of the world [7-10]. It is also

* Corresponding author, e-mail: oleg@icm.krasn.ru

noted that this effect are becoming more significant nowdays. In particular, there is an increase in the rate of growth of temperature differences between urban and rural areas, an increase in the dependence of the effect on the time of year and geographical location of the city. The relationship with population density, building density, traffic density and other characteristics on the UHI in cities on each season and time is also considered [11]. These changes attract increasing attention of urban ecologists and decision-makers of the cities [12, 13].

The assessment of the LST by remote sensing methods is based on thermal infrared (IR) data. Existing satellite systems currently provide IR data with different repeatability and level of detail. In particular, there are data that are taken several times a day with a spatial resolution of 1 km/pixel, and there are data with a resolution of about 100 m/pixel taken once a week. The accuracy of temperature measurement ranges from fractions of a degree to several degrees and it largely depends on the correct assessment of the influence of the atmosphere [14]. The most attractive data in this context is the data from the Landsat satellite series. It Is became popular due to the combination of technical characteristics, the availability of received information, the presence of a long-term archive of observations [15]. The Landsat-8 has been in orbit since 2013. There is thermal infrared scanner (TIRS) mounted on this satellite that captures two channels in the IR band. The recorded data of IR channels can be converted into radio brightness temperature, which, in turn, into the LST [16-18]. An integral part of the final stage is the calculation of the coefficient of emissivity (emission).

A natural limitation of the results obtained is the level of detail of the generated images. The aforementioned Landsat-8 TIRS scanner has a spatial resolution in the IR range of about 100 m/pixel. This accuracy is clearly insufficient for a detailed analysis of the temperature inhomogeneities of the urban environment [19, 20]. One of the possible methods to solve this problem is the use of additional satellite data of higher resolution.

Thermal conditions in Krasnoyarsk urban area

The city of Krasnoyarsk is a large industrial center with unique natural and climatic features, caused by terrain conditions and thermal heterogeneity of the terrain. Krasnoyarsk is classified as having a high potential for atmospheric pollution. The valley-like relief of the terrain, high frequency of fogs and vapor over the Yenisei lead to accumulation of harmful impurities above the main territory of the city.

Krasnoyarsk is located at the junction of three geomorphological countries: the West Siberian Plain, the Central Siberian Plateau, and the Altai-Sayan Mountainous Country. Krasnoyarsk is located on the two banks of the Yenisei River, it has the hilly terrain. Its centre is in the lowland, and on all sides there are hills, the height difference between different parts of the city reaches 150 meters. Construction of hydroelectric power station on the Yenisei River, led to no freezing during the cold season. The air temperature in winter reaches values below –30 °C. As a result, a significant temperature jump is formed in winter: from very low temperatures over the land plots of the city to positive values over the non-freezing water of the Yenisei River. In turn, in the hot summer months, the opposite is true. The well-heated soil of the urban area has a significantly higher temperature compared to the water of the Yenisei, the temperature of which in the city usually does not exceed +10 °C, due to the deep water intake for the Krasnoyarsk HPP, located 40 km from the city.

Thus, the interaction of the two effects of temperature anomalies adversely affects the ecological situation in the city [21]. Therefore, it is important to observe temperature anomalies at different times of the year using remote sensing data, there are ample opportunities for research in this field.

Data processing algorithm

Unlike a number of other satellite data, such as Terra/MODIS, the LST should be calculated from Landsat data. The initial information is contained in Landsat-8 archived data files, which was downloaded through the United States Geological Survey EarthExplorer service. The TIRS data was extracted from these archives. They are represented as the 10^{th} spectral channel of the Landsat-8 satellite data (tif file with the name ending with B10.tif). The temperature data are written in a file by byte in conventional units (raw geodata), each pixel can take a value in the range from 0 to 215.

To get the actual LST, we need to: first convert these conventional units to the values of radiation coming to the sensor, then convert these values on the sensor to the temperature at the upper limit of the atmosphere, and finally, to determine the LST on the basis of the temperature at the upper limit of the atmosphere [22]. It must be noted that there are various methods for assessing the LST, they are the subject of numerous studies. It is possible to assess the influence of the atmosphere in different ways, to apply different algorithms of atmospheric correction. Also, various methods can be used to calculate the emissivity.

Based on the values of these thermal channels, we calculate the value of LST using the formula [23]:

$$T = \frac{T_B}{1 + \left(\frac{\lambda T_B}{c_2}\right)\ln(e)} \tag{1}$$

where T_B [K] is the at-satellite brightness temperature, λ – the wavelength of emitted radiance, $c_2 = hc/s$ [mK] (= $1.4388 \cdot 10^{-2}$), h [Js] – the Planck's constant (= $6.626 \cdot 10^{-34}$), c [ms^{-1}] – the velocity of light (= $2.998 \cdot 10^{8}$), s [J/K] – the Boltzmann constant (=$1.38 \cdot 10^{-23}$), and e – the emissivity of the surface.

At present, there are two main methods for determining the emissivity from the satellite data. The first method uses the classification of objects in the image, where each class is assigned a specific value of the radiation coefficient, tab. 1, and in the second one it is determined on the base of the NDVI index. The first method is easier to use, but its accuracy is limited and depends on the effectiveness of the classification results of the image. The second method has a higher accuracy and allows you to calculate the surface emissivity for each pixel in the image.

Consider the first method in more detail, where the first step is to determine the type of surface, the entire area is divided into four classes: water, open soil, vegetation and buildings. After the classification of the image, each class corresponds to the value of the emission factor, which is presented in tab. 1 (the values used are approximate, since the radiation coefficient of each material must be obtained from the field survey):

Table 1. Correspondence of the land cover classification and the emissivity values

Land surface	Bare oil	Vegetation	Built-up	Water
Emissivity	0.928	0.982	0.942	0.98

The second method has a higher accuracy and allows to calculate the surface radiation coefficient for each pixel of the image. Consider the second method of determining the radiation coefficient based on the normalized vegetation index NDVI. The correct determination of the surface temperature is limited to an accurate knowledge of the emission factor. The relationship between the surface temperature of the earth and NDVI takes into account that vegetation and soils are the main surface:

$$\varepsilon = a + b\ln(\text{NDVI}) \tag{2}$$

where $a = 1.0094$ and $b = 0.047$ are obtained by a regression analysis based on a large dataset.

To determine NDVI, the red spectral ranges and near IR ranges of the spectrum are used:

$$\text{NDVI} = \frac{\rho_{NIR} - \rho_{\text{RED}}}{\rho_{NIR} + \rho_{\text{RED}}} \tag{3}$$

where ρ_{NIR} is the reflection in the near IR and ρ_{RED} is the reflection in the red spectrum range.

We use both mentioned methods (*i. e.* classification-based and NDVI-based) for calculating the emissivity to obtain LST in our study. However, the second one (NDVI-based) can be considered more preferable.

The peculiarity of the study was the combination of satellite data from several spacecraft. The data used in the Landsat-8 IR range need not be supplemented by data from other channels of this satellite, which are necessary for the calculation of the NDVI vegetation index. Another, more detailed images can be used. In this case, it is possible to construct combined images of higher resolution, similar to the widely used approach of increasing image detail using *pan-sharpening* algorithms. In our case, data from the visible and near IR bands of the PlanetScope satellite constellation [24] with a spatial resolution of three meters were used to calculate NDVI.

Results

The materials for the study of the thermal characteristics of the Krasnoyarsk city were Landsat-8 scenes. There are 15 cloudless scenes in the snow-free period from 2013 to 2017 which were selected for analysis: July 7, 2017, August 7, 2017, July 22, 2017, June 29, 2017, june 20, 2017, May 28, 2017, October 27, 2016, September 5, 2016, June 10, 2016, April 23, 2016, July 17, 2015, July 1, 2015, June 8, 2015, May 14, 2015, July 7, 2014, June 18, 2013. For several of these images, the corresponding high-resolution PlanetScope scenes were used for NDVI determination.

The LST was calculated by eq. (1). The resulting temperature values were converted to °C and a temperature map of the land surface was compiled for each survey date. Calculations of the LST were carried out using the QGIS 2.18 software. Semi-automatic classification plug-in (SACP) was used for atmospheric correction of satellite data and further calculations [25].

Due to the fact that temperature anomalies may differ in different seasons of the year, the study was conducted for images grouped by seasons of the year and this approach is widely used in practice [26]. To find the maximum temperature values within the city, all images were distributed over three seasons: summer, spring, and autumn. The boundaries of thermal anomalies were formed independently for spring, summer and autumn images.

In accordance with the previous procedure, a number of different season maps of the LST of Krasnoyarsk and its surroundings were built. It was found that there are two types of thermal anomalies: natural and anthropogenic. A number of thermal islands of different subtypes in the city was found, such as natural hills, areas near large shopping centers, ample parkings, industrial areas of enterprises, areas of thermal pollution by sewage, fig. 1. The anomalies on the natural hills with the southern and south-western exposure of the slope are well discernible, for example, in the Zheleznodorozhny district of Krasnoyarsk.

It was obtained that intense heat radiation is observed from objects made of dense materials with high heat capacity, such as asphalt, concrete and reinforced concrete, stone. The combination of satellite data from several satellites increase the detalization of temperature

maps to the level of individual city blocks. The results show that the areas of residential development, urban forests and parks, roads are well distinguished, fig. 2.

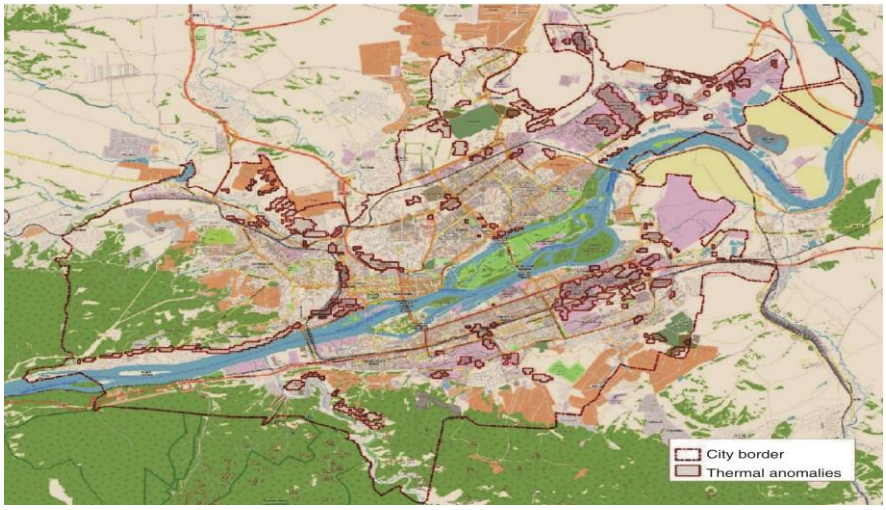

Figure 1. Thermal anomalies in Krasnoyarsk urban area at city level
(*for colour image see journal web site*)

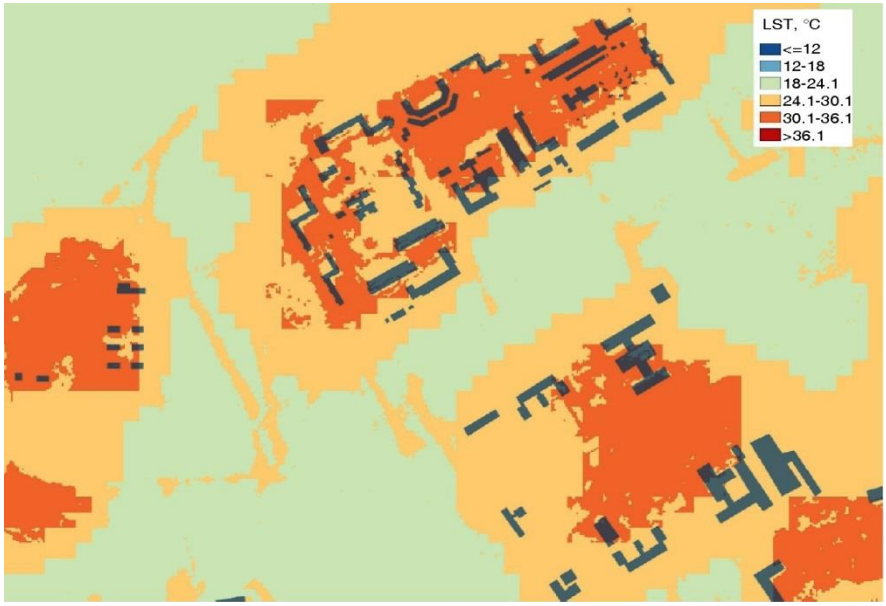

Figure 2. Thermal anomalies at Akademgorodok district of Krasnoyarsk city
(*for colour image see journal web site*)

Conclusions

The use of a combination of satellite data of different spatial resolution makes it possible to conduct a more detailed analysis of temperature anomalies of the urban environment. This information can be used in planning the development of the city, the development of new terri-

tories, the reconstruction of residential and industrial areas, to assess the comfort of living conditions in different urban areas. The formed thermal anomalies are valuable material for future ecological and geographical studies of the territory.

Acknowledgment

This work was carried out with partial financial support from the Russian Foundation for Basic Research and the Government of the Krasnoyarsk Territory (project No. 18-41-242006 p_mk).

References

[1] Stone, Jr., Rodgers, M. O. Urban Form and Thermal Efficiency: How the Design of Cities Influences the Urban Heat Island Effect, *APA Journal*. *67* (2001), 2, pp. 186-198
[2] Sharma, R., Joshi, P., Identifying Seasonal Heat Islands in Urban Settings of Delhi (India) using Remotely Sensed Data – An Anomaly Based Approach, *Urban Climate, 9* (2014), Sept., pp. 19-34
[3] Effat, H., Hassan, O., Change Detection of Urban Heat Islands and some Related Parameters using Multi-Temporal Landsat images – A Case Study for Cairo city, Egypt, *Urban Climate, 10* (2014), Part 1, pp. 171-188
[4] Sheng, L., *et al*., Comparison of the Urban Heat Island Intensity Quantified by Using Air Temperature and Landsat Land Surface Temperature in Hangzhou, *China Ecol. Indicators, 72* (2017), Jan., pp. 738-746
[5] Wang, Y., Akbari, H., Analysis of Urban Heat Island Phenomenon and Mitigation Solutions Evaluation for Montreal, *Sustainable Cities and Society, 26* (2016), Oct., pp. 438-446
[6] Kotharkar, R., *et al*., Urban Heat Island Studies in South Asia: A Critical Review, *Urban Climate, 24* (2018), June, pp. 1011-1026
[7] Peng, S., *et al*., Surface Urban Heat Island across 419 Global Big Cities, *Environmental Science & Technology, 46* (2012), 2, pp 696-703
[8] Peng, J., *et al*., Spatial-Temporal Change of Land Surface Temperature Across 285 Cities in China: An Urban-Rural Contrast Perspective, *Science of The Total Environment, 635* (2018), Sept., pp. 487-497
[9] Imhoff, M. L., *et al*., Remote Sensing of the Urban Heat Island Effect Across Biomes in the Continental USA, *Remote Sensing of Environment, 114* (2010), 3, pp. 504-513
[10] Gaur, A., *et al*., Analysis and Modelling of Surface Urban Heat Island in 20 Canadian cities Under Climate and Land-Cover Change, *Journal of Environmental Management, 206* (2018), Jan., pp. 145-157
[11] Kammuang-Lue, N., *et al*., Influences of Population, Building, and Traffic Densities on Urban Heat Island Intensity in Chiang Mai City, Thailand, *Thermal Science, 19* (2015), Suppl. 2, pp. S445-S455
[12] Taheri Shahraiyni, H., Sodoudi S., High-Resolution Air Temperature Mapping in Urban Areas: A Review on Different Modelling Techniques, *Thermal Science, 21* (2017), 6A, pp. 2267-2286
[13] Vranjes, A., *et al*., Geothermal Concept for Energy Efficient Improvement of Space Heating and Cooling in Highly Urbanized Area, *Thermal Science, 19* (2015), 3, pp. 857-864
[14] Niclos, R., *et la*., Land Surface Air Temperature Retrieval from EOS-MODIS Images, *IEEE Geoscience and Remote Sensing Letters, 11* (2014), 8, pp. 1380-1384
[15] Fu, P., Weng, Q., Consistent Land Surface Temperature Data Generation from Irregularly Spaced Landsat Imagery, *Remote Sensing of Environment, 184* (2016), Oct., pp. 175-187
[16] Windahl, E., Beurs, K., An Intercomparison of Landsat land Surface Temperature Retrieval Methods Under Variable Atmospheric Conditions using in Situ Skin Temperature, *International Journal of Applied Earth Observation and Geoinformation, 51* (2016), Sept., pp. 11-27
[17] Weng, Q., *et al*., Generating Daily Land Surface Temperature at Landsat Resolution by Fusing Landsat and MODIS Data, *Remote Sensing of Environment, 145* (2014), Apr., pp. 55-67
[18] Lu, D., Weng, Q., Spectral Mixture Analysis of ASTER Images for Examining the Relationship between Urban Thermal Features and Biophysical Descriptors in Indianapolis, Indiana, USA, *Rem. Sens. of Env., 104* (2006), 2, pp. 157-167
[19] Stathopoulou, M., Cartalis, C., Downscaling AVHRR Land Surface Temperatures for Improved Surface Urban Heat Island Intensity Estimation, *Remote Sensing of Environment, 113* (2009), 12, pp. 2592-2605
[20] Yang, L., *et al*., Research on Urban Heat-Island Effect, *Procedia Engineering, 169* (2016), Dec., pp. 11-18

[21] Hrebtov, M,. Hanjalić, K., Numerical Study of Winter Diurnal Convection over the City of Krasnoyarsk: Effects of Non-Freezing River, Undulating Fog and Steam Devils, *Bound. Layer Meteo. 163* (2017), 3, pp. 469-495
[22] Giannini, M. B., *et al*., Land Surface Temperature from Landsat 5 TM Images: Comparison of Different Methods Using Airborne Thermal Data, *Journal of Engineering Science and Technology, 8* (2015), 3, pp. 83-90
[23] Weng, Q., *et al*., Estimation of Land Surface Temperature–Vegetation Abundance Relationship for Urban Heat Island Studies, *Remote Sensing of Environment, 89* (2004), 4, pp. 467-483
[24] ***, Planet Team (2017). Planet Application Program Interface: In Space for Life on Earth. San Francisco, Cal., USA, https://api.planet.com
[25] Congedo, L., Semi-Automatic Classification Plugin Documentation, Release 5.3.2.1., Project: Semi-Automatic Classification Plugin, 2016
[26] Ho, H., *et al*., Maximum Urban Air Temperature on Hot Summer days, *Rem. Sens. of Env., 154* (2014), Nov., pp. 38-45

Paper submitted: May 30, 2018
Paper revised: September 3, 2018
Paper accepted: November 1, 2018